Pharm Res (2014) 31:291–304
DOI 10.1007/s11095-013-1160-y

RESEARCH PAPER

Thermosensitive mPEG-*b*-PA-*g*-PNIPAM Comb Block Copolymer Micelles: Effect of Hydrophilic Chain Length and Camptothecin Release Behavior

Xiao-Li Yang • Yan-Ling Luo • Feng Xu • Ya-Shao Chen

Received: 17 April 2013 / Accepted: 28 July 2013 / Published online: 27 August 2013

ABSTRACT

Purpose Block copolymer micelles are extensively used as drug controlled release carriers, showing promising application prospects. The comb or brush copolymers are especially of great interest, whose densely-grafted side chains may be important for tuning the physicochemical properties and conformation in selective solvents, even *in vitro* drug release. The purpose of this work was to synthesize novel block copolymer combs via atom transfer radical polymerization, to evaluate its physicochemical features in solution, to improve drug release behavior and to enhance the bioavailablity, and to decrease cytotoxicity.

Methods The physicochemical properties of the copolymer micelles were examined by modulating the composition and the molecular weights of the building blocks. A dialysis method was used to load hydrophobic camptothecin (CPT), and the CPT release and stability were detected by UV–vis spectroscopy and high-performance liquid chromatography, and the cytotoxicity was evaluated by MTT assays.

Results The copolymers could self-assemble into well-defined spherical core-shell micelle aggregates in aqueous solution, and showed thermo-induced micellization behavior, and the critical micelle concentration was 2.96–27.64 mg L^{-1}. The micelles were narrow-size-distribution, with hydrodynamic diameters about 128–193 nm, depending on the chain length of methoxy polyethylene glycol (mPEG) blocks and poly(N-isopropylacrylamide) (PNIPAM) graft chains or/and compositional ratios of mPEG to PNIPAM. The copolymer micelles could stably and effectively load CPT but avoid toxicity and side-effects, and exhibited thermo-dependent controlled and targeted drug release behavior.

Conclusions The copolymer micelles were safe, stable and effective, and could potentially be employed as CPT controlled release carriers.

KEY WORDS copolymer micelles · cytotoxicity · drug release · stability · thermosensitivity

Electronic supplementary material The online version of this article (doi:10.1007/s11095-013-1160-y) contains supplementary material, which is available to authorized users.

X.-L. Yang • Y.-L. Luo (✉) • F. Xu (✉) • Y.-S. Chen
Key Laboratory of Macromolecular Science of Shaanxi Province
School of Chemistry and Chemical Engineering
Shaanxi Normal University
Xi'an 710062, People's Republic of China
e-mail: luoyanl@snnu.edu.cn
e-mail: fengxu@snnu.edu.cn

INTRODUCTION

Recently, block copolymer micelles as promising hydrophobic drug nanocarriers have been attracting significant attention in drug delivery systems (DDS) (1–3). Their unique core-shell architecture are widely utilized to improve the solubility of hydrophobic drugs and to modulate the pharmacokinetics of these drugs (4). Various copolymer micelles, especially stimuli-responsive copolymer micelles, have currently been prepared, and they show prolonged circulation in the blood compartment and the selective accumulation of micelles at a specific site (5–7). Since lesion issues and tumor cells have a relatively-high temperature than normal tissues, designing thermoresponsive block copolymer micelles is very significant, by which both passive and positive targeting therapeutics can be realized (8,9). In these applications, the stability of the block copolymer micelles is imperative to its ultimate utility as a drug delivery vehicle and is governed by thermodynamic and kinetic principles (10–12). The molecular architecture, chemical nature and length ratio of hydrophilic and hydrophobic blocks are reported to have effect on the micellization behavior and in turn on the related biomedical properties (11,13,14). The copolymers with comb or brush architectures are of great interest, whose densely-grafted side chains may be important for tuning their physicochemical properties and conformation in selective solvents. Their small size, better surface properties, especially desired *in vitro* drug release kinetics and longer circulating period can be

attained by control over the size, composition and functionality of the building blocks.

Camptothecin (CPT) is a kind of potent plant anticancer drugs extracted from camptotheca acuminata targeting intracellular topoisomerase I, and has a short-term curative effect to cancer including primary and metastatic colon carcinoma, small cell lung carcinoma, ovarian, breast, pancreatic, and stomach cancers (4,15–17). Its structure is a planar pentacyclic ring including a pyrrolo[3,4-β]-quinoline moiety, conjugated pyridone moiety and one chiral center within the alpha-hydroxy lactone ring. The planar structure containing the lactone ring is thought to be one of the most important factors in topoisomerase inhibition and cancer therapy. However, the CPT has so far not been successfully used in cancer therapy because of its water insolubility, (high) adverse drug reaction and lactone ring instability (15,16). Studies have demonstrated that the active lactone form of CPT analogs is readily hydrolyzed under physiological conditions (pH = 7.4, 37°C), and the hydrolysis rates are accelerated in the presence of human serum albumin (4,15). The rapid hydrolysis of CPT and CPT analogs in plasma occurs within only a few minutes after intravenous injection. Because of these inadequacies, preparing a water-insoluble CPT delivery carrier becomes increasingly significant. Taking into account the hydrophilic-lipophilic nature of amphiphilic block copolymers as well as core-shell micelle nanostructures formed therefrom in aqueous solution, the copolymer micelle drug carriers will be an important option avoiding these inadequacies.

In the present work, our aim is to tailor-make several comb-like copolymers consisting of methoxy poly(ethylene glycol) (mPEG) blocks and hydrophobic polyacrylate (PA) backbones with thermosensitive poly(N-isopropylacrylamide) (PNIPAM) graft chains, mPEG-*b*-PA-g-PNIPAM, and carefully consider and optimize the factors influencing physicochemical properties of copolymer self-assembly micelles and drug release profiles, including the medium temperature, drug loading and copolymer composition, especially the chain length or molecular weight of mPEG blocks etc. It is anticipated that the new drug carrier system is able to improve the drug solubility and stability *in vivo*, while retaining its anticancer therapeutic efficacy, and thus successfully exploiting polymeric micelles for drug delivery, including micelle stability, drug loading capacity, size, size distribution and incorporation of functionalities.

MATERIALS AND METHODS

Materials and Reagents

Methoxy polyethylene glycol (mPEG), analytical grade, with molecular weight (MW) of 750, 2,000, and 5,000, was supplied by the Sigma-Aldrich (UK), and used after dried under vacuum. 4-Dimethylaminopyridine (DMAP, 98%) and triethylamine (TEA, 98%) was purchased from the Tianjin Fuchen Chem. Reagent Factory (China), and refluxed and distilled over CaH_2. N-isopropylacrylamide (NIPAM, 99%) and methacryloyl chloride (MC, 95%) were provided by the J & K Scientific Ltd., Beijing, China and Aladdin Ind. Corp., Shanghai, China, respectively, and used as received. 2-Hydroxyethanethiol (HESH) as a chain transfer agent was purchased from the Sigma-Aldrich (UK) without further purification. 2,2′-Azobisisobutyronitrile (AIBN) was supplied by the Shanghai Yongzheng Chem. Ind. (China), and purified from 95% ethanol before use. CuCl, 2-bromoisobutyryl bromide (BB, 99%) and tris[2-(dimethylamino)ethyl]amine (Me_6TREN) were purchased from the Sigma-Aldrich (UK) without further purification before use. CH_2Cl_2 was provided from the Sinopharm Chem. Reagent Co. Ltd. and distilled after dried over Na. Tetrahydrofuran (THF), isopropanol (IPA) and dimethylformamide (DMF, 99.5%) were supplied by the Alfa Aesar and used without further purification. Camptothecin (CPT, 98%) was purchased from Shanxi Sciphar Hi-Tech Industry Co. Ltd. (China). All other chemicals were of analytical grade and used directly unless otherwise specified.

Synthetic Procedures

Preparation of mPEG-Br Macroinitiator

Synthesis of macroinitiator mPEG-Br was achieved through a quantitative esterification reaction of mPEG with 2-bromoisobutyryl bromide, and the synthetic route was shown in Scheme 1. Specifically, 1 mmol mPEG was placed in a four-neck flask equipped with a reflux condenser and two constant pressure funnels, followed by 20 ml CH_2Cl_2 and 0.5 mmol (0.0611 g) DMAP as an acylation catalyst. The solution was well stirred and bubbled with dried nitrogen for half an hour to exhaust air. Afterwards, 1.5 mmol (ca 0.19 ml) 2-bromoisobutyryl bromide dissolved in 5 ml dried CH_2Cl_2 in advance was added dropwise within 1 h, accompanied by dried N_2. After the reaction proceeded for half an hour, the solution was cooled in an ice-water bath to 0°C. Then, 1.5 mmol (ca 0.21 ml) TEA dissolved in 1 ml dried CH_2Cl_2 in advance was dropwise added within 1 h through another constant pressure funnel to neutralize the released HBr. The temperature of the reaction mixture solution was elevated to 25°C for another 24 h with stirring (pH ca 7–8). The solution was concentrated by rotary evaporation to remove most of the solvent prior to precipitation into 10-fold anhydrous cold diethyl ether, and then white product was obtained. The product was dried at room temperature in a vacuum oven till constant weight, followed by being dissolved in THF to remove white quaternary ammonium salt through filtration.

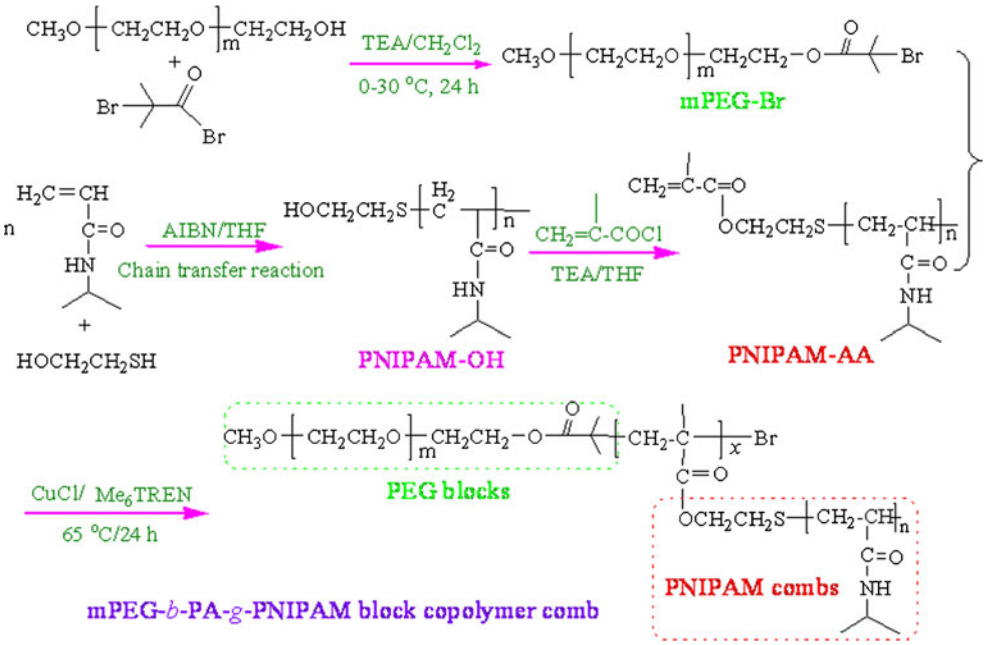

Scheme 1 Schematic illustration of synthesis route of a representative mPEG-*b*-PA-*g*-PNIPAM comb-shaped block copolymer.

The filtrate was again concentrated by rotary evaporation, and then precipitated into 10 fold cold diethyl ether. The mPEG-Br macroinitiator was collected by filtration and dried at room temperature under vacuum till constant weight (yield: 70%). FTIR (v, cm^{-1}): 1,730 (ester C=O stretch), 1,036–1,169 (C-O stretch), 1,395 (−CH_3 bending), 1,458 (−CH_2 bending), 2,880–2,974 (C-H stretch). ^{1}H NMR (300 MHz, $CDCl_3$, δ in ppm): 1.95 (*s*, (BrC($\underline{CH_3}$)$_2$COO-, signal a), 4.33 (*t*, -$CH_2\underline{CH_2}$OOC$(CH_3)_2$CBr, signal b), 3.65 (*t*, -$\underline{CH_2}CH_2$O-, signal c), and 3.38 (*s*, $\underline{CH_3}$O- in PEG chain ends, signal d).

Preparation of PNIPAM-AA Macromonomer

PNIPAM-AA macromonomer was synthesized according to our previous work (18). Hydroxyl-terminated PNIPAM (PNIPAM-OH) was first prepared by a radical polymerization using HESH as a chain transfer agent and AIBN as an initiator. Subsequently, the PNIPAM-AA was attained via esterification reaction between AC and PNIPAM-OH. The MW of the PNIPAM-AA was measured to be 3.72×10^3 by a gel permeation chromatography (GPC) measurement. FTIR (v, cm^{-1}): 3,075 (=C-H stretch), 1,730 (ester C=O), 1,032–1,169 (C-O stretch); 1,648 (C=C stretch and C=O, amide I), 1,550 (v –NH-, amide II), and 3,450 (−NH stretch); 1,366–1,390 (−$CH(CH_3)_2$), 1,458 (−CH_2 bending), 2,880–2,974 (C-H stretch). ^{1}H NMR (300 MHz, $CDCl_3$, δ in ppm): 1.86 (*s*, CH_2=C($\underline{CH_3}$)COO-, signal f), 5.62 (*br*, $\underline{CH_2}$=C(CH_3)COO- in the end ethylene groups of PNIPAM-AA, signal e); 6.50 (br, -$\underline{NH}$-CH$(CH_3)_2$ in PNIPAM), 4.02 (br, *m*, -$\underline{CH}(CH_3)_2$ in PNIPAM side chains, signal l), 2.18–2.69 (br, -$\underline{CH_2}S\underline{CH_2}CH_2$OOC- and -$\underline{CH}$-$CH_2$- in PNIPAM backbones, signals h, h′, h″ and j), 4.25 (*t*, -$CH_2SCH_2\underline{CH_2}$OOC-, signal g), 1.68 (br, -CH-$\underline{CH_2}$- in PNIPAM backbones, signal i), and 1.16 (br, *d*, -CH$(\underline{CH_3})_2$ in PNIPAM side chains, signal m).

Synthesis of Comb Polymer mPEG-b-PA-g-PNIPAM

The thermosensitive mPEG-*b*-PA-*g*-PNIPAM copolymers were synthesized by an atom transfer radical polymerization method using mPEG-Br as macroinitiator and PNIPAM-AA as macromonemer, and the synthetic strategies were shown in Scheme 1. Specifically, 0.02 mmol mPEG-Br and 0.4 mmol PNIPAM-AA were dissolved in IPA/DMSO (2.0/2.0 ml) in a polymerization vial. After the mixture was thoroughly frozen, 0.03 mmol CuCl and 0.03 mmol Me_6TREN were added rapidly. The mixture was degassed by three freeze-pump-thaw cycles. After the bottle was sealed under vacuum, the polymerization reaction was conducted at 60°C for 24 h. The mixture was passed through an activated neutral Al_2O_3 column to remove copper complex. To eliminate possible mPEG-Br residues, the collected polymer was then isolated by dialysis against 1,000 ml deionized water for 72 h, and freeze-dried (mean yield: ca. 46%). FT-IR (v, cm^{-1}): 1,730 (ester C=O), 1,018–1,169 (C-O stretch); 1,648 (C=C stretch and C=O, amide I), 1,550 (v –NH-, amide II), and 3,450 (−NH stretch); 1,366–1,390 (−$CH(CH_3)_2$), 1,458 (−CH_2 bending), 2,880–2,974 (C-H stretch). ^{1}H NMR (300 MHz, $CDCl_3$, δ in ppm): 1.73 (*s*, (−CH_2-C($\underline{CH_3}$)COO-, signal f); 6.62 (br, -$\underline{NH}$-CH$(CH_3)_2$ in PNIPAM, signal k), 3.93 (br, *m*, -$\underline{CH}(CH_3)_2$ in PNIPAM side chains, signal l), 2.08–2.86 (br, -$\underline{CHCH_2}S\underline{CH_2}CH_2$OOC- and -$\underline{CH}$-$CH_2$- in PNIPAM and PA backbones, signals e′, h, h′, h″ and j), 4.15 (*t*, -

$CH_2\underline{CH_2}OO(CH_3)_2C$- and -$CH_2SCH_2\underline{CH_2}OOC$-, signals d and g), 1.57 (br, -CH-$\underline{CH_2}$- in PNIPAM backbones, signal i), and 1.07 (br, *d*, -CH$\underline{(CH_3)_2}$ in PNIPAM side chains, signal m); 1.27 (*s*, (−C$\underline{(CH_3)_2}$COO-, signal a′), 3.58 (*t*, -$\underline{CH_2CH_2}$O-, signal c).

Preparation of Polymer Micelles

Preparation of mPEG-*b*-PA-*g*-PNIPAM polymer micelles was carried out via a dialysis technique. 40 mg copolymer sample was dissolved in 10 ml THF, and then subjected to dialysis against 1,000 ml distilled water using dialysis bags with a molecular weight cut-off (MWCO: 2,000, 5,000, and 7,000 g mol^{-1}, Shanghai Chemical Reagent Co., China, for mPEG750, mPEG2000 and mPEG5000, respectively). The water was replaced hourly for the first 3 h. After dialysis for 72 h, the solution in the dialysis bag was collected and lyophilized for further examination.

Drug Loading and In Vitro Release

Thirty milligrams comb block copolymer and 5 mg CPT were separately dissolved in DMF, and then mixed. The solution was vigorously stirred for 12 h at room temperature and the deionized water was slowly dripped into the solution until micelle formation. The mixture solution was put into a dialysis bag (MWCO: 2000) and subjected to dialysis against 1,000 ml distilled water for 24 h. The solution was centrifuged at 1,000 rpm for 30 min to remove free CPT. The supernatant was filtered with 0.8 μm of syringe filter. To determine the drug loading capacity (LC) and entrapment efficiency (EE), the drug-loaded micelle solution was lyophilized to attain a white powder. The CPT-loaded copolymer sample was then dissolved in DMF and analyzed by UV absorbance at 366 nm using a standard calibration curve (C (mg L^{-1})=(A-0.004)/76.13) experimentally obtained with the CPT/DMF solution (19).

For assessing the CPT release, the lyophilized drug-loaded copolymer (10 mg) was dissolved in 10 ml PBS solution of pH 7.4, and then the solution was placed in the dialysis tube. The dialysis tube was directly immersed into 400 ml PBS solution, and an aliquot of 4 ml solution was withdrawn periodically. The solution volume was kept constant by adding 4 ml PBS solution of pH 7.4 after each sampling. The amount of CPT released from micelles was measured through UV absorbance at 366 nm .

Characterization and Measurements

FTIR and ^{1}H NMR

Fourier transform infrared (FTIR) spectra were recorded on an AVATAR 360 ESP FTIR spectrometer (Nicolet, USA). Samples were pressed into potassium bromide pellets. ^{1}H nuclear magnetic resonance (^{1}H NMR) spectra were recorded on a Varian Unity 300 MHz NMR spectrometer (Bruker Avance, Germany) with $CDCl_3$ as solvents, and TMS as internal standard.

Gel Permeation Chromatography (GPC) Measurement

The molecular weight (MW) and polydispersity index (PDI) of the synthesized copolymers were measured by gel permeation chromatography (GPC, Waters Corp., USA). Chromatographic-grade DMF containing10 mM LiBr was used as eluent at a flow rate of 1.0 ml min^{-1} at 35°C and low-polydispersity polystyrene as calibration standards. The sample solution was filtered through a 0.45 μm needle-type filter (organic, Φ13 mm), and then injected into sample bottles for measurements.

Liquid Chromatography (LC) Measurements

A reverse-phase high-performance liquid chromatography (HPLC, LC-20AT, Shimadzu Corp., Japan) with a gradient elution mode was employed to investigate the protection effect of copolymer micelles on the lactone ring of CPT against its hydrolysis. CPT-loaded copolymer micelles and free CPT were incubated in PBS of pH 7.4 and 37°C at a CPT concentration of 20 μg ml^{-1}. Aliquots of 20 μl were withdrawn each time, followed by immediate reverse-phase HPLC analysis of the lactone and carboxylate forms of CPT operating at a flow rate of 0.3 ml min^{-1}. Chromatographically-pure acetonitrile (ACN) and 0.2% acetic acid were used as the mobile phases. Eluted solutions were immediately measured by absorption at 366 nm by SPD-6AV UV detector.

Determination of Critical Micelle Concentration

Critical micelle concentration (CMC) of the as-synthesized copolymers in aqueous solutions was studied by a surface tension technique according to our previous work (18). Simply, a series of the copolymer solutions with concentrations from 5×10^{-5} to 1×10^{-1} g L^{-1} were prepared to equilibrate at room temperature overnight, and the surface tension was recorded on a DCAT 21 tensiometer (DataPhysics, Germany) using the Wilhelmy plate method. The CMC was estimated from plots of the static surface tension *versus* the logarithm of the concentration.

Transmittance Measurements

Transmittance of the block copolymer in aqueous solution (250 mg L^{-1}) with temperature was measured on a U-3900 UV–vis spectrophotometer (Hitachi, Japan) equipped with an electronic thermostatic cell holder and a temperature controller

at 500 nm. The rate of heat addition was set at 0.5°C min^{-1}, and the apparatus was calibrated using deionized water at 25°C. Sample cell was thermostated at temperature from 25°C to 70°C prior to measurements. The cloud points (CP) or low critical solution temperature (LCST) of the polymer solution was defined as the temperature producing a half decrease of the total decrease in transmittance.

Transmission Electron Microscope (TEM)

The size and morphology of the mPEG-*b*-PA-*g*-PNIPAM copolymers were observed on a JEOL JEM-1210 transmission electron microscope (TEM, Electron Corp., Japan) at an acceleration voltage of 200 kV. TEM samples were prepared by dipping the freshly-prepared micelle solution containing 2 wt% phosphotungstic acid onto a copper grid with carbon films and dried in air before measurement.

Particle Size and Zeta Potential Measurements

The valid diameter and particle size distribution of mPEG-*b*-PA-*g*-PNIPAM micelles (The concentration of micelle solutions is 250 mg L^{-1}) were measured by dynamic light scattering (DLS, BI-90Plus, USA) equipped with an argon ion laser operating at $\lambda = 660$ nm and output power of 15 mW. *Zeta* potentials of the freshly-prepared micelles were measured by the laser particle *zeta* potential detecting instrument (Delsa Nano C, Beckman Coulter, USA) at 25°C. All the measurements were set at a fixed scattering angle of 90°, and simulated physiological temperature for duration of 10 min, and each measurement was repeated three times. An average value was obtained from the three measurements.

X-Ray Diffraction (XRD)

To confirm the CPT loading in copolymer micelles, an X-ray diffraction (XRD, Cu radiation, $\lambda = 0.15418$ nm) measurements were recorded using a Rikagu diffractometer (D/Max2550VB+/PC, Rigaku Corp, Japan) running at 40 kV and 40 mA.

MTT Assays

The cytotoxicity of blank and CPT-loaded copolymer micelles as well as free CPT was determined by the methylthiazolyldiphenyl tetrazolium bromide (MTT) assay against the L929 mouse embryonic fibroblast cells and MDA-MB231 human breast cancer cells successively. Before measurement, a certain amount of the polymer micellar solution was put in the nutrient solution, and cell culture was performed. The two cells were separately seeded in a 96-well plate at a density of 1×10^4 cells $well^{-1}$ overnight and then the plates were incubated in a complete Dulbecco's modified eagle's medium containing 10% hyclone fetal bovine serum (high glucose DMEM) at 37°C in 5% CO_2 atmosphere for 24 h. Then, the culture medium was removed and replaced with 100 μL of the medium containing a dilution of blank and CPT-loaded copolymer micelles as well as free CPT. After culture for another 48 h, the medium was replaced by 100 μL of fresh DMEM, followed by adding 25 μL MTT stock solution to each well. After incubation for 4 h, the supernatant was discarded, and then the obtained blue formazan crystals were dissolved in 150 μL per well of DMSO. For reference purposes, cells were seeded in a fresh culture medium (negative control) under the same conditions. Each assay was performed three times. The optical densities with ($OD_{control}$) and without (OD_{sample}) polymer micelles were measured by a 96-well universal microplate reader (Model 680, Bio-Rad laboratories (UK) Ltd) with wavelength at 490 nm, and the cell viability was calculated in line with the following formula:

$$\text{Cell viability } \% = \left(OD_{samples}/OD_{control}\right) \times 100\% \quad (1)$$

In this assay, the Student's test was used to determine the significance of any pairs of observed differences. Differences were considered statistically significant $p < 0.05$. All quantitative results are reported as mean values ± standard deviation.

RESULTS AND DISCUSSION

Synthesis and Structure of mPEG-*b*-PA-*g*-PNIPAM Comb Copolymers

Three types of amphiphilic block copolymers which were comprised of hydrophilic mPEG segments with different degree of polymerization of 16, 45 and 114 and thermosensitive PA-*g*-PNIPAM blocks have been designed and synthesized. The synthetic route involves three consecutive steps: 1) mPEG-Br macro-initiator was prepared by means of quantitative esterification of hydroxyl-capped mPEG–OH with BB; 2) PNIPAM–AA macromonomer was prepared by radical polymerization of NIPAM using HESH as a chain transfer agent, followed by the esterification reaction of the PNIPAM-OH with MC; 3) mPEG-*b*-PA-*g*-PNIPAM comb copolymer was synthesized through ATRP at a molar ratio of [mPEG-Br]/[macromonomer]/[CuCl]/[Me_6TREN] 1:20:1.5:1.5. The synthesis strategies are demonstrated in Scheme 1. The structure of the comb copolymer was characterized by FTIR and ^{1}H NMR measurements, and detailed analyses are demonstrated in Supplementary Material (see also Figs. S1), and the related assignations are described in the synthesis sections. Particularly, signal a at ca 1.95 ppm attributable to the methyl protons in BrC($\underline{CH_3}$)$_2$COO- disappears, and a new shift signal a′ emerges at about 1.27 ppm due to incorporation of -CH_2-

CH- repeating units from $-CH_2=CH-$ between Br atoms and $-C(CH_3)_2-$. The disappearance of the $\underline{CH_2}=C(CH_3)COO-$ shift signal at 5.62 ppm (signal e) and reinforcement at 2.08–2.86 ppm (signals e′) further illustrates that the $CH_2=C(CH_3)-$ groups have changed into $-CH_2-C(CH_3)-$ main chains due to polymerization, and the mPEG-*b*-PA-*g*-PNIPAM comb copolymers are successfully synthesized. FTIR findings corroborate the above description. Especially, the absorption peaks at 3,450, 1,648, 1,550 and 1,032–1,169 cm^{-1} ascribed to –NH stretch, amide I(C=O), amide II and C-O stretch, respectively, confirm the synthesis of the block copolymers.

The number-average (Mn), weight-average (Mw) molecular weight and polydispersity index (PDI) of copolymers were measured by GPC, as shown in Table I. These comb copolymers have almost identical PNIPAM graft chains from 10 to 12 under an identical [mPEG-Br]/[macromonomer]/[CuCl]/[Me_6TREN]=1:20:1.5:1.5, and the difference is one PNIPAM graft unit based on $mPEG_{45}$-Br. In addition, it can be seen that the Mn of the resultant copolymers is increased, which originates from the macroinitiator mPEG-Br with different Mn and slightly increased PNIPAM unit. GPC elution curves support the above analysis, as shown in Fig. S2 (see Supplementary Material). The GPC traces also show that the copolymers are unimodal and narrow molecular weight distributions, with small PDI values from 1.14 to 1.22, which confirms the successful synthesis of mPEG-*b*-PA-*g*-PNIPAM comb block copolymers by ATRP.

Table I Sample Codes, GPC Data and Various Physicochemical Parameters of the As-Prepared mPEG-*b*-PA-*g*-PNIPAM Block Copolymers in Aqueous Solution

Copolymers Sample codes	$mPEG_{16}$-*b*-PA-*g*-$PNIPAM_{10}$ Polym A	$mPEG_{45}$-*b*-PA-*g*-$PNIPAM_{11}$ Polym B	$mPEG_{114}$-*b*-PA-*g*-$PNIPAM_{12}$ Polym C
mPEG MW	750	2000	5000
Mn	37140	44330	50950
Mw	45260	52660	58010
PDI[a]	1.22	1.19	1.14
CMC[b], mg L^{-1}	2.96	14.90	27.64
LCST[b], °C	44.5	42.0	41.8
TEM diameter[b], nm (Blank)	111.2 ± 8.7	149.9 ± 7.2	161.1 ± 9.6
TEM diameter[b], nm (CPT-loaded)	120.8 ± 7.9	166.7 ± 9.1	178.7 ± 10.4
D_h by DLS[b], nm (Blank)	128.90 ± 4.39	185.40 ± 5.02	192.50 ± 10.10
PDI[c]	0.194 ± 0.011	0.226 ± 0.014	0.291 ± 0.008
D_h by DLS[b], nm (CPT-loaded)	142.50 ± 5.13	209.10 ± 8.53	212.70 ± 12.31
PDI[c]	0.185 ± 0.022	0.211 ± 0.013	0.275 ± 0.013
Zeta potentials[b], mV	−22.79 ± 2.72	−25.49 ± 3.35	−18.42 ± 2.43

[mPEG-Br]/[macromonomer]/[CuCl]/[Me_6TREN]=1:20:1.5:1.5;

[a] Polydispersity index of molecular weight

[b] The copolymer micelle concentration was set at 250 mg L^{-1} and the determination temperature was 25°C;

[c] Polydispersity index of hydrodynamic diameters D_h

Physicochemical Properties of Block Copolymer Self-Assembly Micelles

In this work, we notice that the as-synthesized three mPEG-*b*-PA-*g*-PNIPAM comb copolymers are dissolvable in THF, while they can spontaneously assemble into micelle aggregates in aqueous solution. The CMC of the micelle aggregates as a key parameter representing formation of micelles (20) was determined by a surface tension technique, as shown in Fig. 1a and Table I. It is clear that the CMC values of the three copolymer micelle aggregates are enhanced with increasing the MW of copolymers, especially the MW of the hydrophilic mPEG blocks and PNIPAM grafts. Actually, the decrease in the hydrophilic mPEG chain length is similar to the increase in lengths of hydrophobic PA backbones, which leads to increase in the aggregating tendency of the copolymer micelles. This finding is in agreement with previous work reported by Chang *et al.* (21). This copolymer micelle with a smaller CMC value can form a more stable micellar structure, and thus has higher stability upon strong dilution in the bloodstream. On the other hand, the hydrogen bond interactions between PNIPAM grafts and H_2O molecules also contribute a lot to change in CMC values. The lower MW for $mPEG_{16}$-*b*-PA-*g*-$PNIPAM_{10}$ than the other two copolymers should be responsible for its low CMC to some extent. This indicates that the micelle-forming ability is affected not only by the length of PNIPAM grafts but also by the hydrophilic mPEG chain length.

To confirm whether these micelles exhibit a thermal sensitivity as expected, we further examine the transmittance of polymeric micelle solutions as a function of external temperature, as shown in Fig. 1b, and the calculated LCST values are summarized in Table I. It is noticed that these copolymers exhibit phase transition temperature above 40°C and the LCST is decreased with increasing the molecular weight of mPEG blocks or block copolymers. Although more hydrophilic mPEG chains would result in increase in the LCST, the length or molecular weight of the thermosensitive PNIPAM chains may play an important role in the LCST change. Mendez (22) and Halperin (23) once predicted that the chain density and molecular weight would affect the PNIPAM collapse. Plunkett KN *et al.* (24) found that the chain collapse above the LCST decreases with decreasing grafting density and molecular weight of PNIPAM. This finding well reveals that the high LCST value for the former may be correlated with relatively-short PNIPAM chains, which is not sensitive

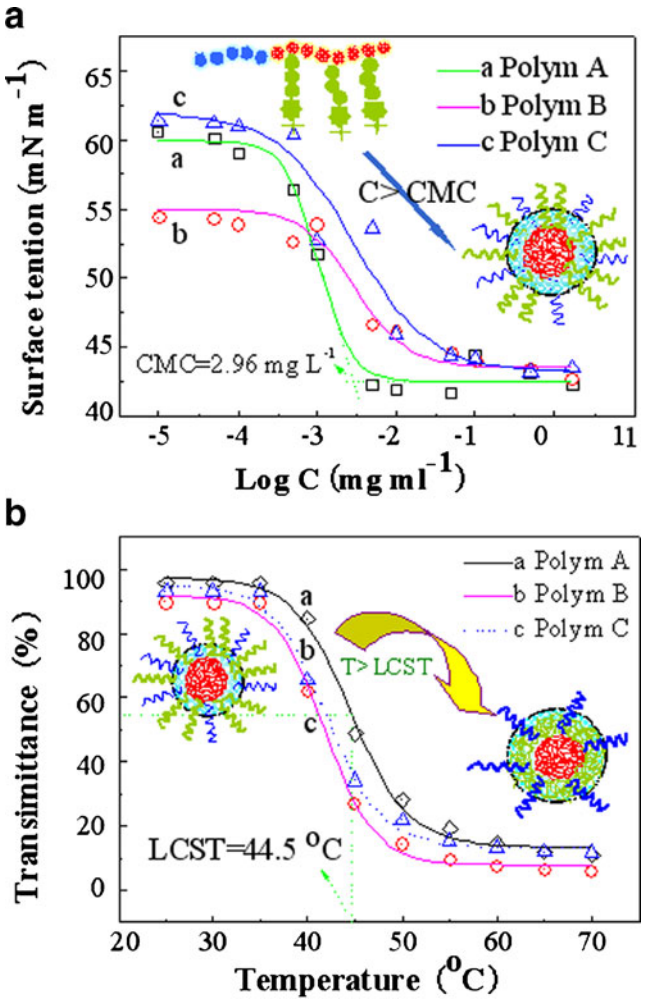

Fig. 1 (**a**) Static surface tension *versus* the logarithm of the copolymer concentration in aqueous solution; and (**b**) Transmittance dependence of the copolymer micelles with concentration of 250 mg L^{-1} in aqueous solution with external temperature.

enough to temperature change in comparison with the latter. Therefore, the LCST can be manipulated by altering the molecular weight of mPEG blocks and the charge feed of the two components. All these LCST values are above 37°C (normal body temperature), which will be meaningful for realizing thermo-triggered active drug targeting release. This LCST can guarantee that the drug-loaded copolymer micelles can maximally prevent drug in the bloodstream from leakage (37°C and pH 7.4) while they quickly deliver drug at tumor tissues or lesion sites, where continuously and fast cell replicating as well as increased metabolic activity raises the temperature of tumor cells. Taking into account a narrow, clinically relevant temperature range of 37–42°C (25), the block copolymer micelles with mPEG MW of 2,000 and 5,000 may be more acceptable and desired, which have LCST of about 42°C, close to a possible ceiling temperature at tumor tissues. These copolymer micelles may spontaneously collapse or contract at tumor cells with slightly higher temperature than LCST, while the thermosensitive micelle with low mPEG MW (750) might aggregate at the tumor sites with the local hyperthermia therapy (42–45°C) (26,27).

The morphologies, size and size distribution were examined by TEM observations and DLS measurements, as displayed in Fig. 2. Both the blank and the CPT-loaded copolymer micelles assume spherical appearance in shape, with PA backbones as an inner core, PNIPAM as a centered shell and mPEG as an outer corona, similar to our previous work (18). The encapsulation of small molecular drug, CPT, has no impact on formation of the copolymer micelle aggregates. The blank copolymer micelles have TEM diameters from ca 110 to 160 nm, while the sizes become large from 120 to 170 nm after the copolymer micelles accommodate some CPT into their cores, as listed in Table I. DLS measurements give similar results, and the blank micelles have hydrodynamic diameters (D_h) from 128 to 193 nm, and the CPT-loaded micelles have D_h from 142 to 213 nm. These findings demonstrate that CPT has been entrapped into the core of the micelles and thus improved the solubility of the hydrophobic drugs. This small particle size can reduce non-selective reticuloendothelial system (RES) scavenge and show enhanced permeability and retention (EPR) effects at solid tumor sites for passive targeting. The particle size is enhanced with increasing the molecular weight of copolymers and/or mPEG blocks and PNIPAM grafts since these hydrophilic segments are fully extended in water. The copolymer micelles are found to be relatively narrow-size-distribution whether the CPT is loaded or not, with polydispersity indexes (*PDI*) from 0.185 to 0.291.

Zeta potential (ζ) is a scientific term for electrokinetic potential in colloidal systems. The significance of zeta potentials is that its value can reflect the stability of colloidal dispersions, and indicate the degree of repulsion between adjacent, similarly charged particles in dispersion. A high zeta potential will confer stability, the solution or dispersion will resist aggregation. When the potential is low, attraction exceeds repulsion and the dispersion will break and flocculate. So, micelles with high ζ potentials are electrically stabilized while micelles with low ζ potentials tend to coagulate or flocculate (28,29). The polymer micelle aggregates are found to have ζ values from about −18 to −25 mV. The negative ζ values of mPEG-*b*-PA-*g*-PNIPAM are explainable with the assumption of a contact potential (18). This contact potential exists between two materials with different permittivity in a way that the material with the lower dielectric constant carries the negative charge. The $mPEG_{45}$-*b*-PA-*g*-$PNIPAM_{11}$ copolymer micelle has the highest ζ absolute value, signifying it has better stability than other two systems. On the other hand, the micelle nanoparticles with more negative charges have more chances to be adsorbed onto platelets acording to the studies by Gu *et al.* (30). Therefore, the $mPEG_{114}$-*b*-PA-*g*-$PNIPAM_{12}$ micelle with the relatively-low ζ value is less possible to be adsorbed,

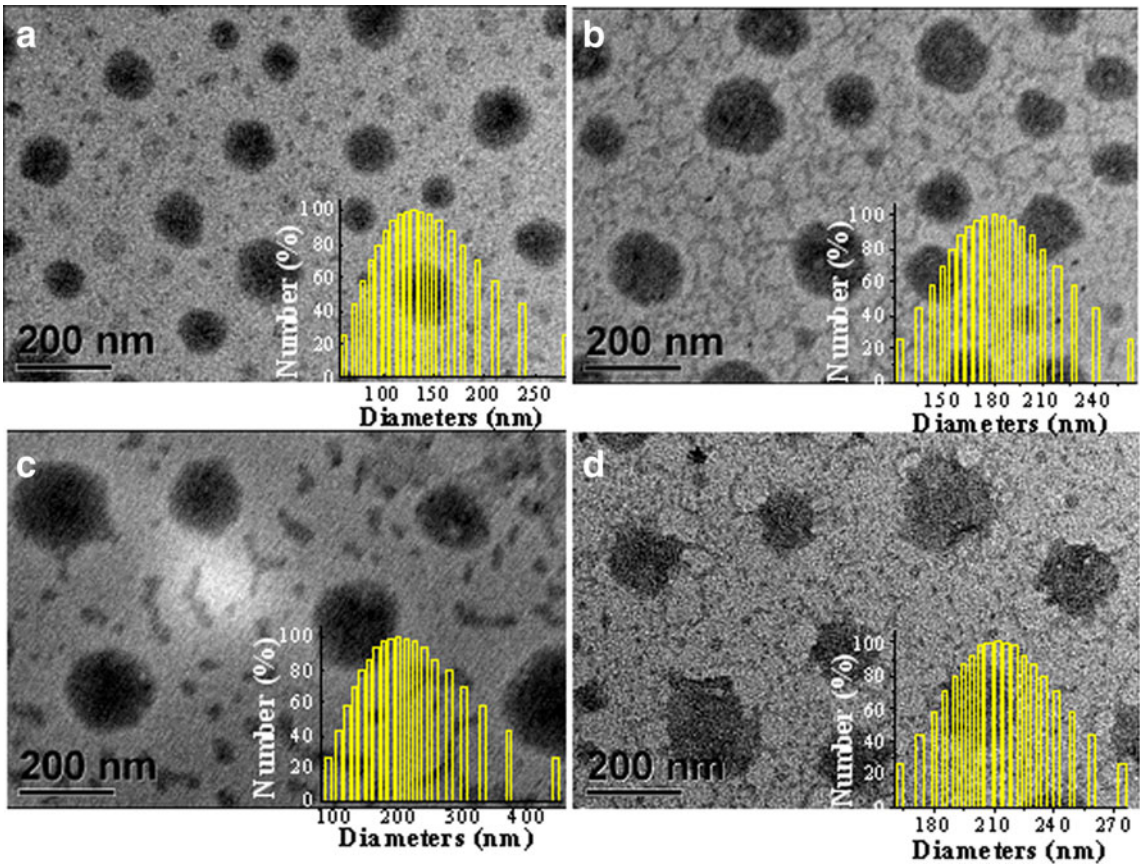

Fig. 2 TEM images of the blank micelles (**a**) Polym A, (**b**) Polym B and (**c**) Polym C, and (**d**) CPT-loaded Polym C micelle. The insets show DLS histograms of particle size distribution of respective copolymer micelles (Copolymer micelle concentration: 250 mg L^{-1}).

which may result in relatively-high drug delivery efficiency. The decreased ζ absolute value may be related to increase in the D_h value (31). Of course, the micelle stability and drug release are affected by other factors such as the steric hindrance and hydrophilic/hydrophobic balance etc., and should comprehensively be taken into account.

XRD Analysis

The physical entrapment of the CPT into the mPEG-*b*-PA-*g*-PNIPAM nanomicelles was achieved by a dialysis technique as described in the experimental part, and its physical status inside the micelles was confirmed by XRD analysis. XRD spectra of free CPT, CPT-loaded $mPEG_{114}$-*b*-PA-*g*-PNIPAM powder and blank $mPEG_{114}$-*b*-PA-*g* -PNIPAM powder are shown in Fig. 3. Free CPT displays a number of sharp peaks at a 2θ range from 10 to 50° in the XRD spectrum, signifying that CPT is a crystalline compound, where some paracrystalline phases appear as narrow peaks. While an amorphous scattering XRD pattern appears at 2θ from 15 to 35° for the blank $mPEG_{114}$-*b*-PA-*g*-PNIPAM sample. In the XRD spectrum of the CPT-loaded $mPEG_{114}$-*b*-PA-*g*-PNIPAM powder, only several specific crystalline or paracrystalline peaks of CPT emerge at 2θ of 19.13–26.13°, and most of the CPT crystalline diffraction peaks disappear or are masked since the CPT is encapsulated into the amorphous copolymer powder, which is in agreement with the result reported by Luo etc. (32). In addition, there are literatures reporting that this change in XRD patterns is ascribed to the fact that the polymer matrices may inhibit the crystallization of CPT, and the CPT partially loses its ordering

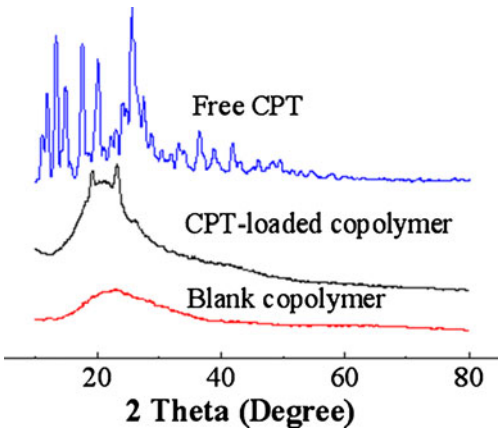

Fig. 3 XRD spectra of free CPT, CPT-loaded $mPEG_{114}$-*b*-PA-*g*-PNIPAM powder and the blank $mPEG_{114}$-*b*-PA-*g*-PNIPAM powder.

(33,34). On the basis of the above analysis, it is deduced that CPT may be predominately present in crystalline or paracrystalline form when the CPT is entrapped into the amorphous $mPEG_{114}$-*b*-PA-*g*-PNIPAM copolymer powder.

Cytotoxicity

Biocompatibility is vital for applications of polymer materials in drug delivery system. To evaluate the *in vitro* cytotoxicity of the as-prepared copolymer micelles and bioactivity of the CPT drug after loading, the MTT assay for the blank and CPT-loaded micelles as well as free CPT has been performed. Figure 4a shows proliferation results of L929 cells treated with the blank and CPT-loaded $mPEG_{45}$-*b*-PA-g-PNIPAM copolymer micelles with concentrations from 1 to 800 mg L^{-1} after 48 h incubation. It is clear from Fig. 4a that the blank copolymer micelles are found to be almost non-toxic even when the concentration of copolymer micelles is as high as 800 mg mL^{-1} with relative cell viabilities above 90%, suggesting the blank copolymer micelles have good biocompatibility. The CPT-loaded polymer micelles (LC: 8.47%) show relatively-lowered cytotoxicity. The cell survival percentage is, however, above 78%, which may be related with a little amount of *in vitro* CPT release. This indicates that the CPT-loaded $mPEG_{45}$-*b*-PA-g-PNIPAM copolymer micelles do not produce remarkable cytotoxicity against normal cells upon performing circulation inside the human body. On the contrary, the free CPT exhibits significantly high cytotoxicity in a dose-dependent manner and even under a fairly low CPT concentration of about 0.1 μg ml^{-1} only 36% cells can survive, which reveals higher inhibition than CPT-loaded copolymer micelles. Therefore, toxicity and side-effects can avoid before the CPT-loaded $mPEG_{45}$-*b*-PA-g-PNIPAM copolymer micelles carry CPT into the lesion sites, while the free drug is potent to produce the desired pharmacological action as the CPT-loaded micelles reach to diseased tissues. It is therefore anticipated that the mPEG-*b*-PA-g-PNIPAAm block copolymer are provided with good biocompatibility.

To further evaluate the potential drug delivery and therapeutic efficacy of CPT, the *in vitro* cytotoxicity of free CPT and CPT-loaded micelles or micelle-released CPT against MDA-MB231 human breast cancer cell lines is also performed, as shown in Fig. 4b. It is clear that the CPT-loaded micelle discloses a comparable inhibition against the MDA-MB231 cell growth in CPT-dose-dependent to free CPT, with the half maximal inhibitory concentration (IC_{50}) of 3.35 μg ml^{-1} (ca 9.19 μM) except the micelle sample with a CPT concentration of 1.0 μg ml^{-1}, which is ascribed to the intracellular release of CPT from the CPT-loaded micelles and subsequent entry into the nuclei of breast cancer cells. The slightly lower cytotoxicity for the CPT-loaded micelles than free CPT under the same CPT concentration may be due to the time-consuming CPT release from the micelles, as depicted in Fig. 5a for Polym B. The *in vitro* cytotoxicity evaluation against the MDA-MB231 human breast cancer cell lines further corroborates the aforementioned conclusion that the CPT released from the copolymer micelles present the desired antitumor activities, and meanwhile avoid the side effects of free CPT.

CPT Loading and *In Vitro* Drug Release Profiles

As stated before, the unique core-shell architecture of amphiphilic block copolymer micelles offers the water-insoluble drug the possibility of entrapping in the hydrophobic cores of the micelles, while the hydrophilic shell provides a stable interface between the hydrophobic core and the aqueous medium, which leads to increase in solubility of hydrophobic drug and effective bioavailability (1,35). The drug loading capacity (LC) and entrapment efficiency (EE) of the block copolymer micelles are estimated by the following equations:

$$\mathrm{LC}(\%) = (\text{Mass of drug in micelles}/\text{Mass of the feeding polymer}) \times 100\% \quad (2)$$

$$\mathrm{EE}(\%) = (\text{Mass of drug in micelles}/\text{Mass of the feeding drug}) \times 100\% \quad (3)$$

In this work, the amount of CPT loaded into the copolymer micelles was determined by UV–vis spectroscopy. The

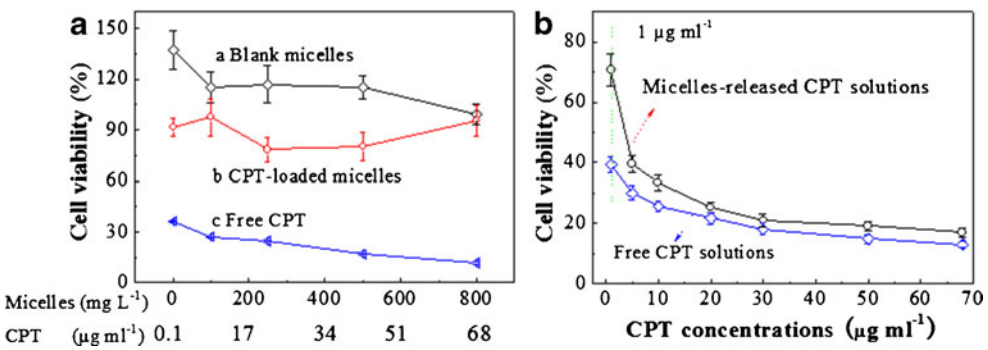

Fig. 4 Cell cytotoxicity of (**a**) the blank and (**b**) drug-loaded $mPEG_{45}$-*b*-PA-*g*-PNIPAM block copolymer micelles (Concentration: 1–800 mg L^{-1}; and LC: 8.47%), as well as (**c**) free CPT (Concentration: 0.126–100.800 μg ml^{-1}) against (**a**) L929 cell lines and (**b**) MDA-MB231 human breast cancer cell lines after 48 h incubation ($n = 3$).

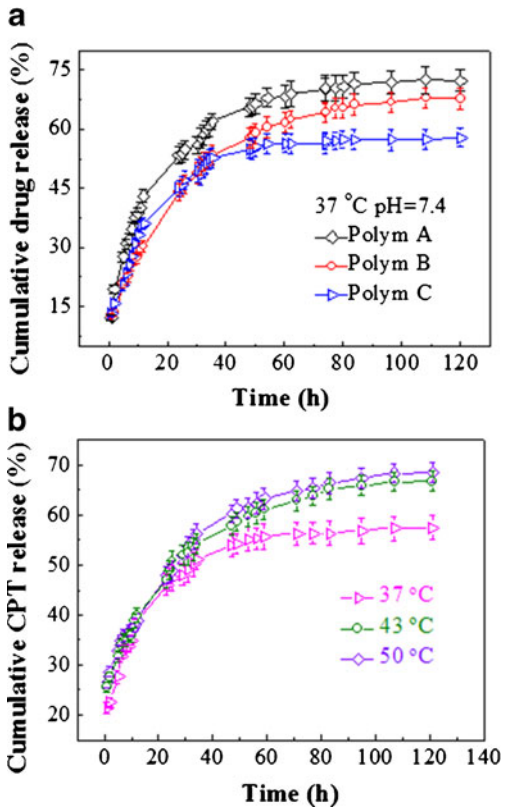

Fig. 5 CPT release profiles from (**a**) three kinds of CPT-loaded copolymer micelles in PBS solution of pH 7.4 at 37°C, and (**b**) $mPEG_{114}$-*b*-PA-*g*-PNIPAM copolymer micelles in PBS solution of pH 7.4 at 37 and 50°C ($n = 3$).

LC and EE of CPT-loaded mPEG-*b*-PA-*g*-PNIPAM copolymer micelle nanoparticles are averagely about 7.89 and 47.40%, respectively. This value matches that of CPT-loaded copolymer micelles nanoparticles with the identical feed ratio of CPT reported elsewhere (36).

Drug delivery from polymeric micelles is influenced by several factors such as nature and size of carrier materials, drug loading capacity and preparation technology, etc., and release is usually a complicated process, involving several mechanisms, such as diffusion of the drug molecules, and degradation and erosion of the polymer matrices (37–39). To validate the feasibility of the as-prepared copolymer micelles as drug targeting carriers, *in vitro* drug release profiles from CPT-loaded copolymer micelles are evaluated by varying temperature and copolymer compositions, as illustrated in Fig. 5. The amount of CPT released from the micelles in PBS solution of pH 7.4 was measured using UV absorbance at 366 nm, and the standard curve was generated in a mixed solution of DMF and PBS solution of pH 7.4 (as little DMF as possible to dissolve CPT) in consideration the water-insolubility of CPT:

$$C\left(mg\ L^{-1}\right) = (A - 0.0046)/75.91 \quad (4)$$

where A is the UV absorbance at 366 nm. The cumulative drug release (*wt*%) was calculated on the basis of the following formula:

$$Cumulative\ drug\ release\ \% = M_t/M_o \times 100 \quad (5)$$

M*t* corresponds to the amount of CPT drug released at time t, and M_0 stands for the amount of CPT loaded in the polymeric micelles.

As indicated in Fig. 5a, the cumulative CPT release under normal physiological conditions (37°C and pH 7.4) is approximately 58, 68 and 72% at a release time of 120 h, which corresponds to Polym C, Polym B and Polym A micelles, respectively. In particular, the $MPEG_{16}$-*b*-PA-*g*-$P(NIPAM)_{10}$ (Polym A) micelle displays the fastest release rate of CPT from the micelles during the whole release process, indicating that the CPT release from the copolymer micelles is closely correlated with copolymer compositions or the length ratio of hydrophilic/hydrophobic blocks. Lower molecular weight of mPEG or shorter mPEG hydrophilic chain gives rise to a faster CPT release dose. This may be the reason that long mPEG hydrophilic chains have better stabilization for the hydrophobic core of micelles, leading to slower CPT release than short hydrophilic blocks.

Furthermore, thermo-triggered CPT release profiles were investigated by using 'Polym C' loaded with CPT at 37 and 43°C based on the aforegoing clinically-relevant temperature range of 37–42°C, and the CPT release at 50°C is used as a control for the external hyperthermia method (25), as depicted in Fig. 5b. The cumulative release of CPT from the $mPEG_{114}$-*b*-PA-*g*-$P(NIPAM)_{12}$ micelle nanoparticles is increased with temperature, and the release amount is 58, 67 and 69% at a release time of 120 h at 37 (T<LCST), and 43 and 50°C (T>LCST), respectively. Higher drug release rate and release amount above LCST than below LCST are probably ascribed to temperature-induced structural alterations of copolymer micelles. Below LCST, the PNIPAM chains are stretched, whose hydrophilicity stabilizes in the micellar core and the CPT is well encapsulated; while above the LCST the PNIPAM chains become more hydrophobic, leading to the shrinkage of the micellar structure and quick diffusion of CPT out of the micelles. Temperature is also a possible factor affecting the diffusion rate of CPT above the LCST since the rate of diffusion is directly proportional to temperature. In addition, the accelerated motion of CPT molecules by the abatement of the hydrophobic interaction between the core and the CPT at higher temperatures is worthy of consideration (40). Since the temperature of tumor tissues/cells or lesion sites is generally higher than normal tissues (41,42), the thermo-induced CPT-loaded copolymer micelles can be utilized to minimize drug leakage *in vivo* under normal physiological conditions of pH 7.4 and 37°C, while they produce

accelerated drug release under tumor or lesion microenvironments. This is very interesting for the copolymer micelles as drug carriers for site-specific release to cancer cells (43,44). It is worth noting that the release temperature is close to or slightly higher than the ceiling temperature of tumor tissues. Therefore, the CPT release from these micelles *in vivo* may be achieved by spontaneously thermo-triggered release at about 42–43°C (>LCST). Viz., the targeted drug release *in vivo* can be attained only at the temperature of tumor cells slightly higher than the LCST. Meanwhile the active targeting release at the tumor sites can also performed through the local hyperthermia therapy at about 42–45°C (25,45), especially in the case of the $mPEG_{16}$-*b*-PA-*g*-$PNIPAM_{10}$ thermosensitive micelle with LCST of 44.5°C. In consideration of the intrinsic heat dissipation in normal tissues due to augmented blood flow, temperatures below 45°C can be maintained even as the temperature of the hyperthermia therapy is set above 45°C, whereas most solid tumors do not have this adaptive capacity and can be heated to 50°C with virtually no injury to normal organs. Therefore, this class of copolymer micelles with proper block degrees of polymerization or copolymer composition may be more suitable for *in vivo* drug release carriers, and the combination of the external hyperthermia method with nanoscaled micelles is feasible for targeting release.

To well understand the hydrophobic drug CPT release behavior, the Ritger-Peppas model (46) is adopted to elucidate the CPT transport mechanism by fitting the above cumulative release data (The model is valid only for the first 60% of the fractional release, i.e., $M_t/M_\infty \leq 60\%$).

$$M_t/M_\infty = kt^n \tag{6}$$

$$ln(M_t/M_\infty) = ln(k) + n\ ln(t) \tag{7}$$

where M_t and M_∞ correspond to the total amount of drug released at time t and equilibrium time, respectively. k is a kinetic constant that reflects the drug release rate and is obtained by measuring the intercepts of the lines by the least square method. n is an exponent characteristic of the release mechanism. When n is ≤0.5, the drug release is controlled by Fickian diffusion. When n is between 0.5 and 1, an anomalous diffusion occurs. As n equals to 1, drug release follows zero-order release. The linear regression results are summarized in Table II. It is seen that at PBS of pH 7.4 and 37°C the release exponent "n" values are decreased with increasing the molecular weights of the comb copolymers or mPEG blocks and PNIPAM grafts, and the n values range from 0.5164 to 0.3483. These data reveal that the CPT release for these formulations complies with different release mechanisms. For 'Polym B' and 'Polym C' formulations, the CPT is released by pure diffusion controlled mechanism (Fickian diffusion) while the n value is slightly beyond 0.5 for 'Polym A', implying that the release mode of CPT loaded in the 'Polym A' micelle somewhat deviates from Fickian diffusion control mechanism. A higher 'n' value in the case of the 'Polym A' formulation than 'Polym B' and 'Polym C' ones implies that the release mode of CPT loaded in the 'Polym A' micelle formulation may be controlled by short lengths of the mPEG hydrophilic chains. The smaller n value ($n<0.5$) at 43 and 50°C than at 37°C only suggest that the CPT release above LCST is remarkably modulated by the Fickian diffusion, and a faster CPT release rate is correlated with the higher kinetic constant k of the drug release from the two formulations (comparing 0.2283 at 43°C and 0.2585 at 50°C with 0.1387 at 37°C). In summary, the results indicate that the CPT release may be affected by Fickian diffusion and thermo-induced conformation alteration.

Table II Regression Equations and Kinetic Parameters Obtained From Fitting Drug Release Experimental Data in PBS of pH 7.4

Samples	T (°C)	Regression equations	R^2	n	ln(k)
Polym A	37	$y = 0.5164x - 2.0837$	0.9952	0.5164	−2.0837
Polym B	37	$y = 0.4386x - 2.2568$	0.9916	0.4386	−2.2568
Polym C	37	$y = 0.3483x - 1.9755$	0.9841	0.3483	−1.9755
Polym C	43	$y = 0.2375x - 1.4772$	0.9776	0.2375	−1.4772
Polym C	50	$y = 0.1637x - 1.3528$	0.9877	0.1637	−1.3528

Stability of CPT Lactone Rings and CPT-Loaded Copolymer Micelles

Antitumor efficacy of CPT as a kind of plant anticancer drugs is closely related with its lactone rings (36). However, the lactone ring in CPT is highly susceptible to hydrolysis. The open ring form is inactive and it must therefore be closed to inhibit topo I. Now that the copolymer micelles can entrap water-insoluble drug into its hydrophobic core, and thus enhance the solubility and stability, the reverse-phase HPLC system is adopted to evaluate the protection effect of copolymer micelles on the lactone ring of CPT against the hydrolysis. Figure 6 shows the ring-opening percentage of the CPT lactone ring of a CPT-7.31*wt*% Polym C micelle with time under physiological condition (pH 7.4, 37°C) at a CPT concentration of 20 μg ml^{-1}. Generally, the lactone ring form of CPT is located at a higher retention time above 9.8 min in analytical HPLC spectra, and the absorption peak of the carboxylate form after hydrolysis is detected at a low retention time below 9.0 min, and these absorption peaks shift with changes in media, drug loading and/or drug concentration in medium etc. (36,47). In this work, it can be seen from Fig. 6 that both free CPT dissolved in the PBS solution and the CPT entrapped in the hydrophobic core of the copolymer micelles give rise to the lactone ring form and carboxylate form of CPT at 7.2 and 13.4 min, respectively. However, unprotected free

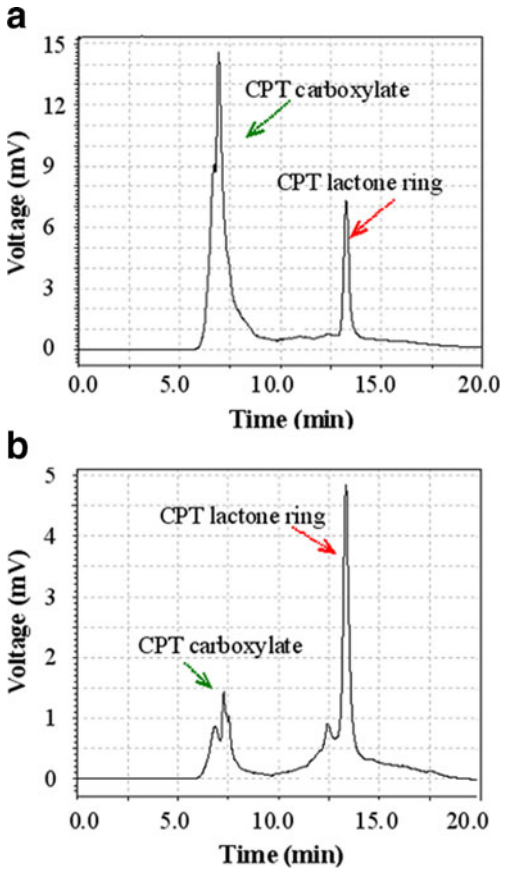

Fig. 6 HPLC chromatograms of (**a**) free CPT and (**b**) CPT-loaded Polym C (mPEG$_{114}$-*b*-PA-*g*-PNIPAM) micelles (Concentration: 275 mg L^{-1}) incubated in PBS solution of pH 7.4 for 48 h at a CPT concentration of 20 μg ml^{-1}.

CPT exhibits an obvious lactone ring opening percentage while the CPT encapsulated in the 'Polym C' micelle demonstrates a decreased ring opening rate. By comparing the relative peak areas obtained from the lactone ring form and carboxylate form of CPT in Fig. 6, free CPT exposed to PBS solution for 48 h is estimated to have hydrolyzed by about 74%. Whereas approximate 71% of CPT still is maintained in the lactone ring form when CPT is loaded in polymer micelles for a long time of 48 h incubation. These findings show that the mPEG-*b*-PA-*g*-PNIPAM micelles effectively protect the active lactone ring from the hydrolysis as previous work (48), and avoid the generation of the inactive CPT hydrolysate carboxylate through hydrolysis, thus exhibiting high stablization.

The physical stability of the copolymer micelles as drug delivery system is crucial for their practical applications, which is affected by various factors from the copolymer micelles and the drug used such as CMC and zeta potentials, glass transition temperature and drug loading, as well as the interactions between the drug and the core-forming block, etc. (49). In general, a hydrophilic/hydrophobic balance of copolymer micelles may be lost as the hydrophobic drugs are entrapped into the hydrophobic cores of the micelles, leading to decrease in the stability of the micelles. To optimize copolymer micelle-based formulations, finding a balance between drug loading and micelle stability is very important. In this work, the stability of CPT-loaded copolymer micelles was monitored and evaluated by changes in the CPT contents (It is defined as ratios of the CPT mass in copolymer micelles at time t to the initial CPT mass encapsulated in copolymer micelles) in copolymer micelles during a storage period of 60 days at 9°C, as illustrated in Fig. 7. It is clearly seen that within the scope of the experiments these CPT-loaded copolymer micelles show some stability with a CPT loss less than 8% after 60 days and no CPT precipitation is observed. This decrease in the CPT contents is probably because of the partial CPT decomposition or slow delivery from the copolymer micelles. In this copolymer micelle-based formulation, only hydrophobic interactions produce between the drug and the hydrophobic block forming core of micelles. However, subtle differences exist among these CPT-loaded copolymer micelles, depending on loading capacities of CPT and copolymer compositions. For a close CPT loading capacity, the CPT-loaded 'Polym B' (LC: 8.47%) shows better stability than the CPT-loaded 'Polym C' (LC: 7.31%), and only about 4.7% CPT is lost for the 'Polym B', and 6% CPT loss for the 'Polym C' after 60 days. The increased CPT loss is correlated with the system composition and the resulting increased CMC value, corresponding to the enhanced MW of mPEG blocks and PNIPAM grafts. In the meanwhile, it is noticed that with the increase in the CPT loading amount (Comparing the two 'Polym B' samples with LC of 8.47 and 13.76%), the CPT loss is increased due to change in the hydrophilic/hydrophobic balance of the micelles and the stability of CPT-loaded copolymer micelles is somewhat decreased. Therefore the CPT-loaded copolymer micelles with a proper CPT loading and copolymer composition seem to be stable during storage. These results demonstrate that it is necessary to optimize the copolymer micelle-based formulations to meet the requirements of the storage stability of the drug-loaded copolymer micelles while maintaining higher LC. Further efforts are made to increase the LC of the hydrophobic

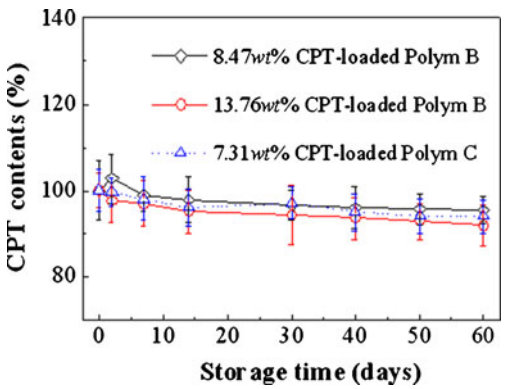

Fig. 7 Changes in CPT contents loaded in the copolymer micelles with various compositions and CPT loading contents in PBS of pH 7.4 at 9°C during a 60-day storage.

anticancer drugs, and preserve long-term stability by decreasing the level of drug degradation to an acceptable range.

CONCLUSION

In summary, a new type of thermoresponsive mPEG-*b*-PA-*g*-PNIPAM copolymer combs has successfully been synthesized, as confirmed by FT-IR, ^{1}H NMR and GPC measurements. The copolymers can spontaneously assemble and form almost spherical nanoscale core-shell micelle aggregates in aqueous solution, with CMC from 2.96 to 27.64 mg L^{-1}, and a mean particle size below 200 nm, as disclosed by surface tension, TEM and DLS determination. The copolymer micelles are confirmed to exhibit the thermo-induced phase transition behavior, with LCST from 40°C to 44.5°C, as revealed by UV–vis measurements. The physicochemical properties are dependent on the length or molecular weight of mPEG blocks and/or copolymer compositions. TEM, DLS, XRD and UV–vis findings prove that CPT is entrapped into the cores of the copolymer micelles, and the stability of the CPT-loaded copolymer micelles depends on the optimization of the CPT-loaded copolymer micelle-based formulations. HPLC analyses show that the encapsulation of the CPT in the copolymer micelles can keep most of the lactone rings stable. The CPT can be continuously delivered from the polymer micelles without the initial burst release, and the CPT release is accelerated when the environmental temperature is raised above the LCST, showing thermo-triggered controlled drug-release properties. Therefore the designed system has enhanced the therapeutic efficiency of unstable CPT with lowest leakage in physiological conditions, and drug toxic side effects could be reduced, as elucidated by the CPT release experiments and MTT assays.

ACKNOWLEDGMENTS AND DISCLOSURES

This work is supported by the Natural Science Foundation of China (grant NSFC 21273142), Natural Science Foundation of Shaanxi Province (2012JM6009), and Graduate Education Innovation Funds (2013CXS049).

REFERENCES

1. Sanada Y, Akiba I, Sakurai K, Shiraishi K, Yokoyama M, Mylonas E, *et al.* Hydrophobic molecules infiltrating into the poly(ethylene glycol) domain of the core/shell interface of a polymeric micelle: evidence obtained with anomalous small-angle X-ray scattering. J Am Chem Soc. 2013;135(7):2574–82.
2. Wang C, Long C, Xie C, Chen X, Zhang L, Chu B, *et al.* Two novel nanoscale preparations of micelle and thermosensitive hydrogel for docetaxel to treat malignant tumor. J Biomed Nanotechnol. 2013;9(3):357–66.
3. Peng J, Qi T, Liao J, Fan M, Luo F, Li H, *et al.* Synthesis and characterization of novel dual-responsive nanogels and their application as drug delivery systems. Nanoscale. 2012;4(8):2694–704.
4. Kawano K, Watanabe M, Yamamoto T, Yokoyama M, Opanasopit P, Okano T, *et al.* Enhanced antitumor effect of camptothecin loaded in long-circulating polymeric micelles. J Control Rel. 2006;112:329–32.
5. Kim DJ, Heo JY, Kim KS, Choi IS. Formation of thermoresponsive poly (N-iso propylacrylamide)/dextran particles by atom transferradical polymerization. Macromol Rapid Commun. 2003;24:517–21.
6. Gil ES, Hudson SM. Stimuli-responsive polymers and their bioconjugates. Prog Polym Sci. 2004;29:1173–222.
7. Alarcon CH, Pennadam S, Alexander C. Stimuli responsive polymers for biomedical applications. Chem Soc Rev. 2005;34:276–85.
8. Rezaei SJT, Nabid MR, Niknejad H, Entezami AA. Multifunctional and thermo-responsive unimolecular micelles for tumor-targeted delivery and site-specifically release of anticancer drugs. Polymer. 2012;53:3485–97.
9. Opanasopit P, Yokoyama M, Watanabe W, Kawano K, Maitani Y, Okano T. Influence of serum and albumins from different species on stability of camptothecin-loaded micelles. J Control Release. 2005;104:313–21.
10. Kim S, Shi Y, Kim JY, Park K, Cheng JX. Overcoming the barriers in micellar drug delivery: loading efficiency, in vivo stability, and micelle-cell interaction. Expert Opin Drug Del. 2010;7:49–62.
11. Rapoport N. Physical stimuli-respons ive polymeric micelles for anticancer drug delivery. Prog Polym Sci. 2007;32:962–90.
12. Attia ABE, Ong ZY, Hedrick JL, Lee PP, Ee PLR, Hammond PT, *et al.* Mixed micelles self-assembled from block copolymers for drug delivery. Cur Opin Colloid Interface Sci. 2011;16:182–94.
13. Konovalov MA, Kramarenko EY, Khokhlov AR, Reineker P. Conformational behavior of diblock comb copolymers. J Chem Phys. 2009;130:164903–9.
14. Zhao J, Mountrichas G, Zhang G, Pispas S. Thermoresponsive core–shell brush copolymers with poly(propylene oxide)-block-poly(ethylene oxide) side chains via a 'grafting from' technique. Macromolecules. 2010;43(4):1771–7.
15. Li X, Kong X, Zhang J, Wang Y, Wang Y, Shi S, *et al.* A novel composite hydrogel based on chitosan and inorganic phosphate for local drug delivery of camptothecin nanocolloids. J Pharm Sci. 2011;100(1):232–41.
16. Tang DL, Song F, Chen C, Wang XL, Wang YZ. A pH-responsive chitosan-*b*-poly(p-dioxanone) nanocarrier: formation and efficient antitumor drug delivery. Nanotechnology. 2013;24(14):145101–10.
17. Lu J, Liong M, Li Z, Zink JI, Tamanoi F. Biocompatibility, biodistribution, and drug-delivery efficiency of mesoporous silica nanoparticles for cancer therapy in animals. Small. 2010;6(16):1794–805.
18. Luo YL, Wei Y, Xu F, Zhang LL. Novel thermo-responsive self-assembly micelles from a double brush-shaped PNIPAM-g-(PA-b-PEG-b-PA)-g-PNIPAM copolymer via an atom transfer radical polymerization route. J Polym Sci, Part A: Polym Chem. 2012;50(10):2053–67.
19. Wei H, Zhang XZ, Cheng C, Cheng SX, Zhuo RX. Self-assembled, thermosensitive micelles of a star block copolymer based on PMMA and PNIPAAm for controlled drug delivery. Biomaterials. 2007;28:99–107.
20. Venkataraman S, Hedrick JL, Ong ZY, Yang C, Ee PLR, Hammond PT, *et al.* The effects of polymeric nanostructure shape on drug delivery. Adv Drug Del Rev. 2011;63:1228–46.
21. Chang YC, Chu IM. Methoxy poly(ethylene glycol)-*b*-poly(valerolactone) diblock polymeric micelles for enhanced encapsulation and protection of camptothecin. Eur Polym J. 2008;44:3922–30.
22. Mendez S, Curro JG, McCoy JD, Lopez GP. Computational modeling of the temperature-induced structural changes of tethered poly(N-isopropylacrylamide) with self-consistent field theory. Macromolecules. 2005;38:174–81.

23. Halperin A. Compression induced phase transitions in PEO brushes: the n-cluster. Model Eur Phys J B. 1998;3:359–64.
24. Plunkett KN, Zhu X, Moore JS, Leckband DE. PNIPAM Chain collapse depends on the molecular weight and grafting density. Langmuir. 2006;22(9):4259–66.
25. Dreher MR, Simnick AJ, Fischer K, Smith RJ, Patel A, Schmidt M, *et al.* Temperature triggered self-assembly of polypeptides into multivalent spherical micelles. J Am Chem Soc. 2008;130(2):687–94.
26. Cai Q, Zhang L, Yang J, Jin R. Core-crosslinked poly(N-isopropyl - acrylamide-co-N, N-dimethylacrylamide)-b-poly(ε-caprolactone) micelles for paclitaxel thermo-sensitive controlled release behaviors. J Clin Rehabilitative Tissue Eng Res. 2010;14(29):5505–10.
27. Lee SC, Chang JY. Thermosensitive block copolymers consisting of poly(*N*-isopropylacrylamide) and star shape oligo(ethylene oxide). Bull Korean Chem Soc. 2009;30(7):1521–5.
28. Greenwood R, Kendall K. Selection of suitable dispersants for aqueous suspensions of zirconia and titania powders using acoustophoresis. J Eur Ceramic Soc. 1999;19:479–88.
29. Hanaor D, Michelazzi M, Leonelli C, Sorrell CC. The effects of carboxylic acids on the aqueous dispersion and electrophoretic deposition of ZrO2. J Eur Ceramic Soc. 2012;32:235–324.
30. Gu JC, Qiao MX, Gao W, Zhao XL, Hu HY, Xu J, *et al.* Preparation of adriamycin-loaded temperature/pH sensitive self-assembly block copolymer micelles. Acta Pharm Sin. 2009;44:793–7.
31. Tauer K, Gau D, Schulze S, Völkel A, Dimova R. Thermal property changes of poly(N-isopropylacrylamide) microgel particles and block copolymers. Colloid Polym Sci. 2009;287:299–312.
32. Luo Y, Li L, Wang Y, Chan G, Hou Z, Zhang Q. Preparation and characteristic of hydroxycamptothecin-loaded PLA nanoparticles using dialysis method. J Xiamen University Nat Sci. 2010;49(6):832–7.
33. Swaminathan S, Pastero L, Serpe L, Trotta F, Vavia P, Aquilano D, *et al.* Cyclodextrin-based nanosponges encapsulating camptothecin: physicochemical characterization, stability and cytotoxicity. Eur J Pharm Biopharm. 2010;74:193–201.
34. Yao R, Liu L, Deng S, Ren W. Preparation of carboxymethylchitosan nanoparticles with acid-sensitive bond based on solid dispersion of 10-hydroxycamptothecin. ISRN Pharm. 2011;2011:1–9. doi:10.5402/2011/624704.
35. Hevus I, Modgil A, Daniels J, Kohut A, Sun C, Stafslien S, *et al.* Invertible micellar polymer assemblies for delivery of poorly water-soluble drugs. Biomacromolecules. 2012;13:2537–45.
36. Min KH, Park K, Kim YS, Bae SM, Lee S, Jo HG, *et al.* Hydrophobically modified glycol chitosan nanoparticles-encapsulated camptothecin enhance the drug stability and tumor targeting in cancer therapy. J Control Release. 2008;127:208–18.
37. Jaskari T, Vuorio M, Kontturi K, Manzanares JA, Hirvonen J. Iion-exchange fibers and drugs: an equilibrium study. J Control Release. 2001;70:219–29.
38. Freiberg S, Zhu XX. Polymer microspheres for controlled drug release. Int J Pharm. 2004;282:1–18.
39. Opanasopit P, Yokoyama M, Watanabe M, Kawano K, Maitani Y, Okano T. Block copolymer design for camptothecin incorporation into polymeric micelles for passive tumor targeting. Pharm Res. 2004;21:2001–8.
40. Huang XJ, Xiao Y, Lang MD. Self-assembly of pH-sensitive mixed micelles based on linear and star copolymers for drug delivery. J Colloid Interface Sci. 2011;364:92–9.
41. Luo YL, Wang SH, Li ZQ. Characterization, microstructure, and gas sensitive response behavior of PEG/lithium salt polymer electrolyte films. J Mater Sci. 2008;43:174–84.
42. Yahara T, Koga T, Yoshida S, Deguchi T, Shirouzu K. Relationship between microvessel density and thermographic hot areas in breast cancer. Surg Today. 2003;33:243–8.
43. Akimoto J, Nakayama M, Sakai K, Okano T. Temperature-induced intracellular uptake of thermoresponsive polymeric micelles. Biomacromolecules. 2009;10:1331–6.
44. Akimoto J, Nakayama M, Sakai K, Okano T. Thermally controlled intracellular uptake system of polymeric micelles possessing poly(*N*-isopropylacrylamide) -based outer coronas. Mol Pharm. 2010;7:926–35.
45. Huang P, Zhou J. The enhancement of hypeffhermia study on patient with tumor. Modern Oncology. 2010;18(7):1460–2.
46. Ritger PL, Peppas NA. A simple equation for description of solute release I. Fickian and non-Fickian release from non-swellable devices in form of slabs, sphere, cylinders or discs. J Control Release. 1987;5:23–36.
47. Martins SM, Wendling T, Goncalves VMF, Sarmentoa B, Ferreira DC. Development and validation of a simple reversed-phase HPLC method for the determination of camptothecin in animal organs following administration in solid lipid nanoparticles. J Chromatography B. 2012;880:100–7.
48. Greish K, Fang J, Inutsuka T, Nagamitsu A, Maeda H. Macromolecular therapeutics: advantages and prospects with special emphasis on solid tumour targeting. Clin Pharmacokinet. 2003;42:1089–105.
49. Liu J, Lee H, Allen C. Formulation of drugs in block copolymer micelles: drug loading and release. Curr Pharm Des. 2006;12(36):4685–701.